Advances in Nano Research, *Vol. 18, No. 2 (2025) 195-203*
https://doi.org/10.12989/anr.2025.18.2.195

Tube diameter versus frequency: Smart monitoring system based on single walled carbon nanotubes

Emad Ghandourah*

Department of Nuclear Engineering, Faculty of Engineering, King Abdulaziz University, Jeddah, Saudi Arabia

(*Received November 15, 2024, Revised February 4, 2025, Accepted February 6, 2025*)

Abstract. In this study, vibrations of armchair (5, 5) single walled carbon nanotubes (SNTs) have been investigated based on orthotropic model. The influence of the tube diameter is investigated for four different boundary conditions. The frequencies are higher for higher tube diameter. Effect of two different wave number varying the tube diameter values is presented. As the tube diameter increases, the frequency first rises and reaches its maximum value. These kinds of frequencies are crucial to the stability of carbon nanotubes. It has been observed that frequencies rise as wave numbers decrease. Compared to simply supported and simply supported frequency boundary conditions, the clamped-clamped curves are larger. The CNTs are more stable the more the tube foundation can withstand a load from physical circumstances.
Keywords: approximate technique; governing equation; tube diameter; wave numbers; wave propagation

1. Introduction

The investigation of carbon nanotube vibrations is a crucial facet of structural dynamics studies. These tubes have a variety of geometric shapes, including spherical, cylindrical, elliptical, and classical forms. Cylindrical tubes are essential components in many practical domains. Carbon nanotubes are used in a variety of engineering and industrial applications, including building construction, missile technology, and aircraft (Wang *et al*. 2025a, b). Iijima (1991) first reported on carbon nanotubes, which have potential use in material reinforcement, aerospace, medical, defense, and microelectronic devices, among other domains (Sosa *et al*. 2014, Fakhrabadi *et al*. 2015). It has been demonstrated that the conventional molecular dynamics (MD) method outperforms other methods used in the area of atomic modeling, such as ab-initio and tight-binding MD (Iijima *et al*. 1996, Hernandez *et al*. 1998, Qian *et al*. 2002). The computational capabilities of continuum mechanics (Yoon *et al*. 2003, Ansari *et al*. 2011) to produce findings of vast range systems in the nanoscale range is the primary reason it became a notable technique. Because applied mathematics and studies of free vibration evolution are closely related.

The mathematician Galileo (1638) presented his vibration research of structural parts and, by solving problems of the natural frequency type, demonstrated how the length of a simple pendulum depends on its length. Subsequently, he completed the experimental results by incorporating the vibrations of plates and strings. He was not allowed to write in mathematical formulations at the time since the mathematical approach was brief in those days. The incredible pace at which nanoscience and nanotechnology are developing is reflected in the growing number of scientific studies. Iijima (1991) made the discovery of carbon nanotubes (CNTs), which have applications in many different sectors, including material science. The notable computational proficiency and precision of nonlocal models render them a desirable option for future developments in the discipline. Two significant shell theories that have been widely applied in the study of the static and dynamic properties of CNTs are Donnell (1996) and Flügge (1962). Flügge shell theory shows great promise for producing extremely accurate advances to study CNTs. Yoon and Mioduchowski (2003) studied the vibration of single walled carbon nanotubes (SNTs) and multi walled carbon nanotubes (MNTs) using classical Euler-Bernoulli beams. Zhang *et al*. (2005) investigated the vibrational behavior of two-walled carbon nanotubes using the Euler-Bernoulli model (EBM). Yoon (2006) presented a novel approach to the investigation of SNTs. Additionally, modified Timoshenko beams are used to establish various properties of (MNTs). The natural frequencies are recovered through propagation. Recent research has focused as much on double-walled carbon nanotubes (DNTs) as SWNTs due to their widely used mechanical, electrical, and thermal properties. A study on the transverse and torsion waves for CNTs using the nonlocal shell model was reported by Hu *et al*. (2008). The nested CNT tubes with double walls were modeled by Xu *et al*. (2008) as individual elastic beams. According to their research, CNT remained unchanged under specific edge conditions at a given invariable frequency.

In 2008, Tylikowski introduced the layered shell model, nonlocal Euler-Bernoulli, and Galerkin-type finite element techniques for presenting vibration in composite structures. The study conducted by Natsuki *et al*. (2010) examined the

*Corresponding author, Associate Professor, Ph.D.,
E-mail: eghandourah@kau.edu.sa;
emademal@hotmail.com

ISSN: 2287-237X (Print), 2287-2388 (Online)

different lengths of inserted DNTs in the outer and inner tubes. The vibrational properties of a viscous fluid transporting DNTs under clamped-clamped and clamped-free conditions were investigated by Ponnusamy and Amuthalakshmi (2013). Tai *et al*. (2024) utilized the UAVs transmission for Information Based URLLC. In the framework of Sanders-Koiter thin shell theory, which is based on the Rayleigh-Ritz method employing clamped and free edge conditions, Strozzi *et al*. (2014) postulated the low frequency of SNTs. A number of CNT types with varying aspect ratios are investigated in detail. Wang and Wang (2013) employed nonlocal Timoshenko beam theory to study the vibration of carbon nanotubes immersed in an elastic medium. The Timoshenko beam model was based on the idea of nonlocal elasticity.

Xiaoming *et al*. (2025) investigated the magneto-electro elastic plate for the dispersion effect with Lamb wave. Their study carefully investigated the relationship between the critical buckling stress and the chirality, vibrational mode, and aspect ratio of SNTs. Besseghier *et al*. (2015) introduced the Winkler-type model (WTM) for the nonlinear vibration of zigzag SNTs. The energy-equivalent model was used to get the general equation. Ebrahimi and Mahmoodi (2018) provided the static analysis of SNTs and the vibration of CNTs using Eringen's beam theory. The bending moment and strain function was performed under a variety of boundary conditions. Wang *et al*. (2024) identified the longitudinal aerodynamics wind tunnel virtual flight. Zeng *et al*. (2024) studied the effects of vortex pump during the multi-cultivation. Bensattalah *et al*. (2019) investigated the vibration response of SNTs using the TBM. The coupled solution was obtained to observe the frequency influence of SNTs wave mode and chirality.

Additionally, the impact of the aspect ratio on the small scale coefficient is examined. Wang *et al*. (2023) introduced the curve identification for the informed network without calibration. Jena *et al*. (2020) employed the shear deformation beam theory to observe the vibration of SNTs. This new theory has fewer variables than the deformation theory. The magnetic field contains these tubes. The impact of tubing thread connectors seal ability was evaluated by Yu *et al*. in 2022. Fatahi-Vajari *et al*. (2019) used second order PDEs to study the torsional vibration of SNTs. For input saturation, Xu *et al*. (2024, 2025) looked at the PDE-ODE system. Meng *et al*. (2024 a, b) conducted the measures of streamer of insulation surface for embedded electrode. Cao *et al*. (2024) explored the conducted the synergy effect of syngas explosion. Malikan and Eremeyev (2020) used the Winkler matrix with various boundary conditions to predict the buckling analysis of CNTs. The hardness and softness-stiffness of the carbon nanotubes were measured using Hamilton's concept. Lin *et al*. (2024) investigated entropy aspects in industrial load identification. Eringen's and heat conduction theories were used by Pourasghar *et al*. (2021) to illustrate the transient heat conduction and vibration of SNTs. Heat conduction theory's nonlocal term was used to determine the energy scale.

The behavior of SNTs wrapped in DNA was examined by Miyashiro and associates in 2021. Numerous applications, including drug administration, bioimaging, and biosensing in lipid membranes, are pertinent to this work. Ebrahimi (2022) used simply supported conditions to study the intricacies of carbon nanotube vibration based on nonlocal theory. The Rung-Kutta method (RKM) is used to solve the governing equations of motion. Ghasemi and Gouran evaluated the vibration of SNTs packed with fluid and situated on the Pasternak foundation in 2022. The differential equations are solved using the DTM.

Continuum mechanics has also been used to investigate a number of aspects of tiny and nanoscale objects, including thermomechanical studies (Ansari *et al*. 2011, Ebrahimi and Mahmoodi 2018) and CNT buckling (Wang *et al*. 2006, Xu *et al*. 2008, Hu *et al*. 20008). A variety of nonlinear modeling techniques have been employed recently by various researchers (Safaei *et al*. 2019, Benmansour *et al*. 2019, Akbaş 2020, Forsat *et al*. 2021, Luo *et al*. 2022, Moradi *et al*. 2023, Yang *et al*. 2024, Wang *et al*. 2024, Ipek *et al*. 2023, Sedighi and Daneshmand 2014, Jena *et al*. 2020). For the purpose of calculating fundamental natural frequency of SNTs, an orthotropic model with wave propagation has been constructed. The investigation focuses on the impact of four distinct edge conditions and varying wave numbers on the foundation of armchair (5, 5) SNTs. Plotting the frequency fluctuations against tube diameters while varying two distinct wave numbers is done. First, the frequency rises and reaches its peak.

2. Single walled carbon nanotubes (SNTs)

In theory, a graphene sheet is rolled to create single walled carbon nanotubes (SNTs). Three essential structural types of carbon nanotubes: zigzag, armchair, and chiral. In this study, the vibration of armchair is considered (See Fig. 1). The thickness of the nanotube shell is not well defined in the case of nanotubes. Nonetheless, several relations that can be applied in Eq. (1) are provided in the literature. The relation in Eq. (1) relations is taken from (Tokyo, 1995).

$$m = \rho A = 2.4 \times 10^{-24} d \left(\frac{Kg}{nm}\right) \tag{1}$$

$$\tilde{E}\tilde{I} = 428.48d^2 - 397.08d + 109.24 \left(\frac{Kgnm^3}{s^3}\right) \tag{2}$$

The diameter of a nanotube, denoted by d, can be computed using a relation based on the translation indices (n, m).

$$d = 2\tilde{R} = \dot{a}_0 \sqrt{\frac{3(m^2 + n^2 + nm)}{\pi}} \tag{3}$$

where Å is the length of the carbon-carbon bond.

3. Governing equations of CNTs

Single walled carbon nanotubes (SNTs) are made up of rolled graphene sheets that are formed like hexagonal cells. The shell revolution method is used to study the geometry of SNTs. Thus, the mid surface is linked to kinematic notions.

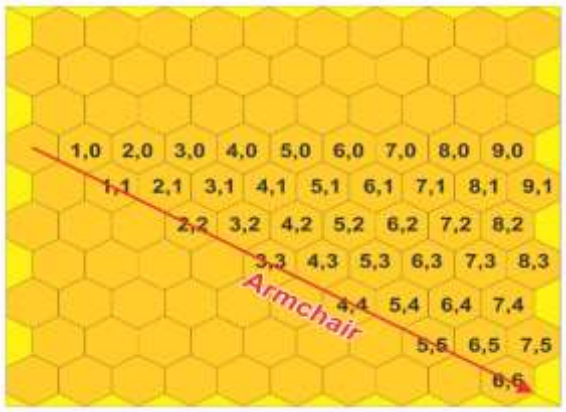

Fig. 1 Armchair CNTs hexagonal representation on the graphene sheet

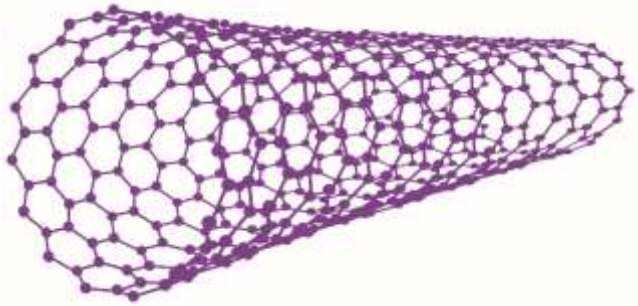

Fig. 2 Rolling graphene sheet look like a hollow cylinder

3.1 Relationship between stress and strain

The stress strain relationship is given as

$$\tilde{\delta}_{\dot{x}} = \frac{\tilde{E}_{\dot{x}}}{[1-\Im_{\dot{x}}\Im_{\phi}]}\left[\tilde{\mu}_{\dot{x}} + \Im_{\dot{x}}\tilde{\mu}_{\phi}\right] \tag{4}$$

$$\tilde{\delta}_{\phi} = \frac{\tilde{E}_{\phi}}{[1-\Im_{\dot{x}}\Im_{\phi}]}\left[\tilde{\mu}_{\varphi} + \Im_{\phi}\tilde{\mu}_{\dot{x}}\right] \tag{5}$$

$$\tilde{\eta}_{\dot{x}\phi} = \tilde{\lambda}_{\dot{x}\phi}\tilde{G}_{\dot{x}\phi} \tag{6}$$

3.2 Strain-displacement relationships

The straightforward mathematical formulas for strain-displacement and curvature-displacement relations. The following is the expression for the relations for strain-displacements

$$\tilde{\mu}_{\dot{x}} = \frac{\partial\tilde{u}}{\partial\dot{x}} \tag{7}$$

$$\tilde{\mu}_{\phi} = \frac{\partial\tilde{v}}{\tilde{R}\partial\phi} - \frac{\tilde{w}}{\tilde{R}} \tag{8}$$

$$\tilde{\lambda}_{\dot{x}\phi} = \frac{\partial\tilde{u}}{\tilde{R}\partial\phi} + \frac{\tilde{v}}{\tilde{X}} \tag{9}$$

3.3 Equations of motion

The general equations of motion for an arbitrary SNT in terms of forces $\dot{x}$, ϕ and $\dot{z}$ directions are in equilibrium.

$$\frac{\partial\tilde{N}_{\dot{x}}}{\partial\dot{x}} + \frac{1}{\dot{r}}\frac{\partial\tilde{N}_{\phi\dot{x}}}{\partial\phi} + \tilde{Q}_{x} = \frac{1}{\dot{r}}\rho\dot{h}\frac{\partial^2\tilde{u}}{\partial t^2} \tag{10}$$

$$\frac{\partial\tilde{N}_{\phi\dot{x}}}{\partial\dot{x}} + \frac{1}{\dot{r}}\frac{\partial\tilde{N}_{\phi}}{\partial\phi} + \tilde{Q}_{\dot{y}} = \frac{1}{\dot{r}}\rho\dot{h}\frac{\partial^2\tilde{v}}{\partial\dot{t}^2} \tag{11}$$

$$\frac{\tilde{N}\phi}{\dot{r}} + \dot{r}\tilde{Q}_{\dot{z}} = \rho\dot{h}\frac{\partial^2\tilde{w}}{\partial\dot{t}^2} \tag{12}$$

The longitudinal modulus of elasticity is denoted by $\tilde{\mu}_{\dot{x}}$, while the circumferential modulus is represented by $\tilde{\mu}_{\phi}$. Similarly $\Im_{\dot{x}}$ is poison's ratio in longitudinal direction and $\Im_{\phi}$ is in circumferential direction.

$$\tilde{N}_{\dot{x}} = \int_{-\frac{\dot{h}}{2}}^{\frac{\dot{h}}{2}} \tilde{\delta}_{\dot{x}} d\dot{z} \tag{13}$$

$$\tilde{N}_{\phi} = \int_{-\frac{\dot{h}}{2}}^{\frac{\dot{h}}{2}} \tilde{\delta}_{\phi} d\dot{z} \tag{14}$$

$$\tilde{N}_{\dot{x}\phi} = \int_{-\frac{\dot{h}}{2}}^{\frac{\dot{h}}{2}} \tilde{\eta}_{\dot{x}\phi} d\dot{z} \tag{15}$$

By putting values of $\tilde{\delta}_{\dot{x}}$, $\tilde{\delta}_{\phi}$ and $\tilde{\eta}_{\dot{x}\phi}$ from Eqs. (4)-(6) in Eqs. (13)-(15) and simplifying, the relation is obtained as

$$\tilde{N}_{\dot{x}} = \frac{\tilde{E}_{\dot{x}}\dot{h}}{[1-\Im_{\dot{x}}\Im_{\dot{\theta}}]}\left(\frac{\partial\tilde{u}}{\partial\dot{x}} + \Im_{\dot{x}}\left[\frac{1}{\tilde{R}}\frac{\partial\tilde{v}}{\partial\phi} - \frac{\tilde{w}}{\tilde{R}}\right]\right) \tag{16}$$

$$\tilde{N}_{\phi} = \frac{\tilde{E}_{\phi}\dot{h}}{(1-\Im_{\dot{x}}\Im_{\phi})}\left[\frac{1}{\tilde{R}}\frac{\partial\tilde{v}}{\partial\phi} - \frac{\tilde{w}}{\tilde{R}} + \Im_{\phi}\frac{\partial\tilde{u}}{\partial\dot{x}}\right] \tag{17}$$

$$\tilde{N}_{\dot{x}\phi} = \tilde{G}_{\dot{x}\phi}\dot{h}\left(\frac{1}{\tilde{R}}\frac{\partial\tilde{v}}{\partial\phi} + \frac{\partial\tilde{v}}{\partial\dot{x}}\right) \tag{18}$$

Using values of $\tilde{N}_{\dot{x}}$, $\tilde{N}_{\phi}$, and $\tilde{N}_{\dot{x}\phi}$ in Eqs. (10)-(12), then following equations are achieved

$$\begin{aligned}&\frac{\partial}{\partial\dot{x}}\left(\frac{\tilde{E}_{\dot{x}}\tilde{R}\dot{h}}{1-\Im_{\dot{x}}\Im_{\phi}}\left(\frac{\partial\tilde{u}}{\partial\dot{x}} + \Im_{\dot{x}}\left[\frac{1}{\dot{r}}\frac{\partial\tilde{v}}{\partial\phi} - \frac{\tilde{w}}{\dot{r}}\right]\right)\right)\\ &+\frac{\partial}{\partial\phi}\left(\tilde{G}_{\dot{x}\phi}\dot{h}\left[\frac{1}{\dot{r}}\frac{\partial\tilde{u}}{\partial\phi} + \frac{\tilde{v}}{\dot{x}}\right]\right) + \dot{r}\tilde{Q}_{\dot{x}} = \rho\dot{h}\frac{\partial^2\tilde{u}}{\partial\dot{t}^2}\end{aligned} \tag{19}$$

$$\begin{aligned}&\frac{\partial}{\partial\dot{x}}\left(\tilde{G}_{\dot{x}\dot{\theta}}\dot{r}\dot{h}\left[\frac{1}{\tilde{R}}\frac{\partial\tilde{u}}{\partial\phi} + \frac{\tilde{v}}{\dot{x}}\right]\right)\\ &+\frac{\partial}{\partial\phi}\left(\frac{\tilde{E}_{\phi}\dot{h}}{(1-\Im_{\dot{x}}\Im_{\phi})}\left[\frac{1}{\dot{r}}\frac{\partial\tilde{v}}{\partial\phi} - \frac{\tilde{w}}{\dot{r}} + \Im_{\phi}\frac{\partial\tilde{u}}{\partial\dot{x}}\right]\right)\\ &+\dot{r}\tilde{Q}_{\dot{y}}\frac{\partial\tilde{v}}{\partial\phi} = \rho\dot{h}\frac{\partial^2\tilde{v}}{\partial\dot{t}^2}\end{aligned} \tag{20}$$

$$\frac{1}{\dot{r}^2}\frac{\tilde{E}_{\phi}\dot{h}}{(1-\Im_{\dot{x}}\Im_{\phi})}\frac{\partial\tilde{v}}{\partial\phi} - \left[\frac{1}{\dot{r}}\frac{\tilde{E}_{\phi}\dot{h}}{(1-\Im_{\dot{x}}\Im_{\phi})} + \dot{r}^2\tilde{S}_{\dot{x}\phi}\tilde{G}_{\dot{x}\phi}\tilde{C}_0\right]\frac{\widetilde{w}}{\dot{r}} + \dot{r}\tilde{Q}_{\dot{z}} = \rho\dot{h}\frac{\partial^2\widetilde{w}}{\partial\dot{t}^2} \tag{21}$$

The longitudinal modulus $\tilde{E}_{\dot{x}}$ can be used to compute the effective bending stiffness along the longitudinal direction $\widetilde{K}_{\dot{x}}$ and the effective thickness $\dot{h}_0$ = 1.6 nm and equivalent thickness of $\dot{h}$ = 2.7. In this case, the axial coordinate, angular coordinate, axial displacement, circumferential displacement, inward deflection and density are represented as $\dot{x}, \phi, \tilde{u}, \tilde{v}, \widetilde{w}$ and $\dot{\rho}$. The radius of the SNTs is $\dot{r}$, while the tube's thickness is $\dot{h}$.

3.4 Relationship between Poisson ratios and Young's modulus

The longitudinal and circumferential Young's modulus are $\tilde{E}_{\phi}$, $\tilde{E}_{\dot{x}}$. Poisson ratios in circumferential and longitudinal direction are denoted by $\Im_{\phi}$, $\Im_{\dot{x}}$.

$$\frac{\tilde{E}_{\phi}}{\tilde{E}_{\dot{x}}} = \frac{\Im_{\phi}}{\Im_{\dot{x}}} \tag{22}$$

In plane stiffness in longitudinal direction $\tilde{S}_{\dot{x}}$, circumferential direction $\tilde{S}_{\phi}$ and in plane shear $\widetilde{K}_{\dot{x}\phi}$.

$$\tilde{S}_{\dot{x}} = \frac{\tilde{E}_{\dot{x}}\dot{h}}{1-\Im_{\dot{x}}\Im_{\phi}} \tag{23}$$

$$\tilde{S}_{\phi} = \frac{\tilde{E}_{\phi}\dot{h}}{1-\Im_{\dot{x}}\Im_{\phi}} \tag{24}$$

$$\tilde{S}_{\dot{x}\phi} = \tilde{G}_{\dot{x}\phi}\dot{h} \tag{25}$$

where $\tilde{G}_{\dot{x}\phi}$ shear modulus in $\dot{x}\phi$ plane.

Furthermore effective bending stiffness is represented by $\widetilde{K}_{\dot{x}}$, $\widetilde{K}_{\phi}$ and $\widetilde{K}_{\dot{x}\phi}$ respectively (Flügge 2013).

$$\widetilde{K}_{\dot{x}} = \frac{\tilde{E}_{\dot{x}}\dot{h}_0^3}{12(1-\Im_{\dot{x}}\Im_{\phi})} \tag{26}$$

$$\widetilde{K}_{\dot{x}\phi} = \frac{\tilde{G}_{\dot{x}\phi}\dot{h}_0^3}{12} \tag{27}$$

$$\widetilde{K}_{\phi} = \frac{\tilde{E}_{\phi}\dot{h}_0^3}{12(1-\Im_{\dot{x}}\Im_{\phi})} \tag{28}$$

The numerical value of $\widetilde{K}_{\dot{x}} = 3.12\times10^{-19}nm$ which is found by taking $\tilde{E}_{\dot{x}} = 1GPa$ and $\Im_{\dot{x}} = 0.3$.

$$\tilde{\Omega} = \frac{\tilde{S}_{\phi}}{\tilde{S}_{\dot{x}}} = \frac{\tilde{E}_{\phi}}{\tilde{E}_{\dot{x}}} = \frac{\widetilde{K}_{\phi}}{K_{\dot{x}}} = \frac{\Im_{\phi}}{\Im_{\dot{x}}} \tag{29}$$

and

$$\widetilde{\mho} = \frac{\tilde{G}_{\dot{x}\phi}}{\tilde{E}_{\dot{x}}} \approx \widetilde{\mho} = \frac{\tilde{G}_{\dot{x}\phi}}{\tilde{E}_{\dot{x}}(1-\Omega\Im_{\dot{x}}^2)} = \frac{\tilde{S}_{\dot{x}\phi}}{\tilde{S}_{\dot{x}}} = \frac{\widetilde{K}_{\dot{x}\phi}}{\widetilde{K}_{\dot{x}}} \tag{30}$$

The relationship between the electro-magnetic effect and elastic deformation can be represented using Lorentz's law $\dot{q} = \tilde{A}\times\tilde{B}$, the Lorentz body force can be shown to be a two-dimensional vector$\dot{q} = \left(\tilde{A}_{\dot{x}}\hat{\imath} + \tilde{A}_{\dot{x}}\hat{\jmath}\right)\times\tilde{B}_{\dot{z}}\hat{k}$, so the values of $\tilde{Q}_x$ and $\tilde{Q}_y$ is given as

$$\tilde{Q}_{\dot{x}} = -\left(\frac{2\tilde{\delta}_x(1-\Im_{\dot{x}}\Im_{\phi})\tilde{S}_{\dot{x}}\tilde{C}_0}{(3-\Im_{\dot{x}})\tilde{E}}\right)\frac{\partial\tilde{u}}{\partial\tilde{x}} \tag{31}$$

$$\tilde{Q}_{\dot{y}} = \frac{2\delta_x(1-\Im_{\dot{x}}\Im_{\phi})\tilde{C}_0\tilde{S}_{\dot{x}\phi}}{(3-\Im_{\phi})\tilde{E}}\frac{\partial\tilde{v}}{\partial\phi} - \rho\dot{g} \tag{32}$$

Therefore, the elasticity model depends on four material parameters $\tilde{E}_{\dot{x}}$, $\Im_{\dot{x}}$, $\tilde{\Omega}$ and $\widetilde{\mho}$.

Using

$$\dot{\lambda} = \frac{1}{12}\left(\frac{\dot{h}^3{}_0}{\dot{h}\dot{r}^2}\right) \tag{33}$$

$$\tilde{\psi}_{\dot{x}} = \frac{\tilde{S}_{\dot{x}}\tilde{C}_0}{(3-\Im_{\dot{x}})\tilde{E}} \tag{34}$$

$$\tilde{\psi}_{\theta} = \frac{\tilde{C}_0\tilde{S}_{\dot{x}\phi}}{(3\mho-\Im_{\dot{x}})\tilde{E}} \tag{35}$$

The longitudinal sound speed is written as

$$\tilde{T}_L = \sqrt{\frac{1}{\dot{\rho}\dot{h}}(\tilde{S}_x)} \approx \sqrt{\frac{1}{\dot{\rho}}(\tilde{S}_x)} \tag{36}$$

Equations of SNTs in the form of three partial differential equations are obtained by using Eqs. (19)-(21) and the foregoing results of Eqs. (23)-(36).

$$\begin{aligned}&\frac{\partial^2\dot{u}}{\partial\dot{x}^2} + \frac{1}{\dot{r}^2}\widetilde{\mho}(1+\dot{\lambda})\frac{\partial^2\tilde{u}}{\partial\phi^2} + \frac{1}{\dot{r}}\left(\tilde{\Omega}\Im_{\dot{x}} + \widetilde{\mho}\right)\frac{\partial^2\tilde{v}}{\partial\dot{x}\partial\phi}\\ &-\frac{1}{\dot{r}}\tilde{\Omega}\Im_{\dot{x}}\frac{\partial\widetilde{w}}{\partial\dot{x}} + \dot{r}\dot{\lambda}\frac{\partial^3\widetilde{w}}{\partial\dot{x}^3} - \frac{1}{\dot{r}}\widetilde{\mho}\dot{\lambda}\frac{\partial^3\widetilde{w}}{\partial\dot{x}\partial\phi^2}\\ &-2\tilde{\delta}_{\dot{x}}\tilde{\psi}_{\dot{x}}\frac{\partial\tilde{u}}{\partial\dot{x}} = \left(\frac{1}{\tilde{T}_{\dot{L}}}\right)^2\frac{\partial^2\tilde{u}}{\partial\dot{t}^2}\end{aligned} \tag{37}$$

$$\begin{aligned}&\tilde{\Omega}\frac{\partial^2\tilde{v}}{\partial\dot{x}\partial\phi} + \widetilde{\mho}(1+3\dot{\lambda})\frac{\partial^2\tilde{v}}{\partial\dot{x}^2} + \left(\tilde{\Omega}\Im_{\dot{x}} + \widetilde{\mho}\right)\dot{r}\frac{\partial^2\tilde{u}}{\partial\dot{x}\partial\phi}\\ &-\tilde{\Omega}\frac{\partial\widetilde{w}}{\partial\phi} + \dot{\lambda}\left(\tilde{\Omega}\Im_{\dot{x}} + 3\widetilde{\mho}\right)\dot{r}^2\frac{\partial^3\widetilde{w}}{\partial\dot{x}^2\partial\phi}\\ &+(2\tilde{\delta}_{\dot{x}}\tilde{\psi}_{\varphi}\Omega\dot{r}^2 - \dot{\rho}\dot{g})\frac{\partial\tilde{v}}{\partial\phi} = \left(\frac{\dot{r}}{\tilde{T}_{\dot{L}}}\right)^2\frac{\partial^2\tilde{v}}{\partial\dot{t}^2}\end{aligned} \tag{38}$$

$$\begin{aligned}&\tilde{\Omega}\Im_{\dot{x}}\frac{\partial\tilde{u}}{\partial\dot{x}} - \dot{\lambda}\dot{r}^2\frac{\partial^3\tilde{u}}{\partial\dot{x}^3} + \dot{\lambda}\widetilde{\mho}\frac{\partial^3\tilde{u}}{\partial\dot{x}\partial\phi^2} + \frac{1}{\dot{r}}\tilde{\Omega}\frac{\partial\tilde{v}}{\partial\phi}\\ &-\dot{\lambda}\left(\tilde{\Omega}\Im_{\dot{x}} + 3\widetilde{\mho}\right)\dot{r}\frac{\partial^3\tilde{v}}{\partial\dot{x}^2\partial\phi} - \dot{\lambda}\dot{r}^3\frac{\partial^4\widetilde{w}}{\partial\dot{x}^4}\\ &-\frac{1}{\dot{r}}2\dot{\lambda}\left(\tilde{\Omega}\Im_{\dot{x}} + 2\widetilde{\mho}\right)\frac{\partial^4\widetilde{w}}{\partial\dot{x}^2\partial\phi^2}\\ &-\frac{1}{\dot{r}}\tilde{\Omega}\dot{\lambda}\left(\frac{\partial^4\widetilde{w}}{\partial\phi^4} + 2\frac{\partial^2\widetilde{w}}{\partial\phi^2} + \widetilde{w}\right)^2\\ &-\frac{1}{\dot{r}}\tilde{\Omega}\widetilde{w} + \tilde{\psi}_{\dot{x}\phi}\tilde{C}_0 = \dot{r}\left(\frac{1}{\tilde{T}_{\dot{L}}}\right)^2\frac{\partial^2\widetilde{w}}{\partial\dot{t}^2}\end{aligned} \tag{39}$$

Table 1 Variation of frequencies with aspect ratios in Tera Hertz (Zhang *et al*. 2009)

		f (THz)				
	Aspect Ratio	17.3	20.89	24.5	28.07	31.64
Clamped-free	MD simulation (Zhang *et al*. 2009)	0.01831	0.01381	0.00916	0.0069	0.0061
	Present	0.01812	0.01332	0.00821	0.0032	0.0011
	TBM (Zhang *et al*. 2009)	0.02041	0.01401	0.0102	0.00777	0.00612
	Present	0.02011	0.01387	0.0090	0.00721	0.00601

Table 2 Variation of frequencies with aspect ratios in Tera Hertz (Kumar 2018)

		f (THz)					
	Aspect ratio	10	12	14	16	18	20
Simply supported	Kumar (2018)	0.4683	0.32527	0.23899	0.18298	0.14467	0.11716
	Present	0.4653	0.32432	0.23732	0.18198	0.14329	0.11538
Clamped-clamped	Kumar (2018)	1.06406	0.73683	0.54256	0.41371	0.32654	0.26546
	Present	1.06399	0.73592	0.54189	0.41284	0.32654	0.26487

Table 3 Variation of frequencies with aspect ratios in Tera Hertz (Naidu *et al*. 2012)

		f (THz)				
	Aspect ratio	16	17	18	19	20
Clamped-free	Naidu *et al*. (2012)	0.0667	0.0591	0.0527	0.0473	0.0427
	Present	0.0621	0.0554	0.0521	0.0434	0.0411
Simply supported-free	Naidu *et al*. (2012)	0.0421	0.0373	0.0333	0.0299	0.0269
	Present	0.0401	0.0353	0.0302	0.0287	0.0232

It is assumed that the three modal displacements functions $\tilde{u}(\dot{x},\phi,\dot{t})$, $\tilde{v}(\dot{x},\phi,\tilde{t})$ and $\tilde{w}(\dot{x},\phi,\dot{t})$, have forms that divide the independent variables. The time variable is shown by $\dot{t}$ and the axial and circumferential coordinates are indicated by $\dot{x}$, ϕ respectively. Thus, the following are the postulated expressions for the displacements due to modal deformation:

$$\tilde{u}(\dot{x},\phi,\dot{t}) = \xi_1 \check{I}(\dot{x}) \cos n\phi e^{i\dot{\chi}\dot{t}} \quad (40)$$

$$\tilde{v}(\dot{x},\phi,\tilde{t}) = \xi_2 \check{J}(\dot{x}) \sin n\phi e^{i\dot{\chi}\dot{t}} \quad (41)$$

$$\tilde{w}(\dot{x},\phi,\dot{t}) = \xi_3 \breve{K}(\dot{x}) \cos n\phi e^{i\dot{\chi}\dot{t}} \quad (42)$$

where $\check{I}(\dot{x})$, $\check{J}(\dot{x})$ and $\breve{K}(\dot{x})$ in the longitudinal, tangential, and radial axes, respectively, and denote the axial modal dependency. A complex exponential function provides the axial modal dependence functions, which are as follows:

$$\check{I}(\dot{x}) = \check{J}(\dot{x}) = \breve{K}(\dot{x}) = e^{-i\zeta_\tau \dot{x}} \quad (43)$$

These three vibration amplitude coefficients in each of the three directions are ξ_1, ξ_2 and ξ_3. The natural angular frequency is shown by $\dot{\chi}$and the circumferential wave number is represented as $\dot{p}$. The formula $\dot{f} = \dot{\chi}/2\pi$ links this frequency to the fundamental frequency. Now, by substituting the expressions for $\tilde{u}$, $\tilde{v}$ and $\tilde{w}$ given in Eqs. (40)-(42) with the conjunction of Eq. (43) into Eqs. (37)-(39) along with their partial derivatives, the frequency equation in the form of eigen value is obtained. The computer software utilized for the numerical values. Where ς_τ is the vibrating carbon nanotube's axial wave number and is directly correlated with the type of boundary conditions that are applied to the ends of SNTs and $n$shows the number of axial half-waves.

4. Results and discussions

The frequency spectrum of armchair (5, 5) single walled carbon nanotubes (SNTs) is examined using modified elasticity shell theory. The explicit expression of the importance of tube diameters versus frequency (THz). Nonlocal models are a desirable option for future developments in the discipline due to their notable computational proficiency and accuracy. Because of the clamped-free boundary condition and fixed length, it is discovered that the frequencies of chiral SNTs are extremely similar. Poisson ratio (= 0.19), mass density (= 2.3 g/cm^3) (Benzair *et al*. 2008), and the equivalent thickness of CNTs (= 0.34 nm) (Zhang *et al*. 2009) are the parameters chosen from previous research. MD simulation is used to determine the SNTs' Young's modulus (Zhang *et al*. 2009). Tables 1-3 presents a comparison of frequency with Zhang *et al*. (2009), Kumar (2018), and Naidu *et al*. (2012). As a result, the natural frequencies calculated by the model that is being given have a high rate of convergence and are supported by analytical, numerical, and experimental results. The current model's findings are found to be highly supported by published research.

Fig. 3 exhibits variations of the natural frequencies (THz) for of armchair (5, 5) SNTs versus tube diameter, *d*. The natural frequency rises as *d* grows, while the frequencies fall as the tube diameter with clamped free boundary

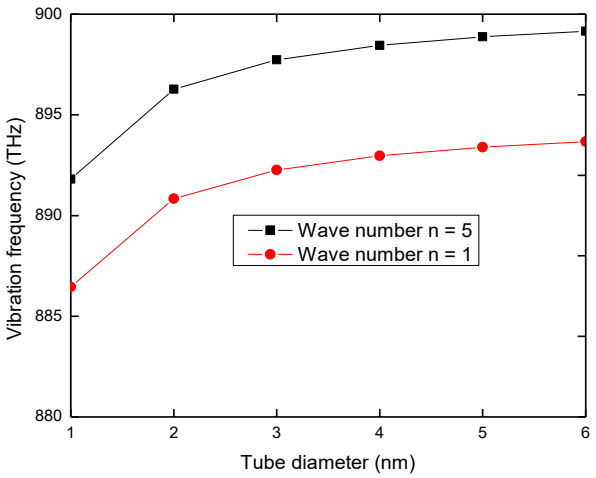

Fig. 3 Response of vibration frequencies (THz) of armchair (5, 5) versus variation of tube diameter (nm) with clamped free edge condition

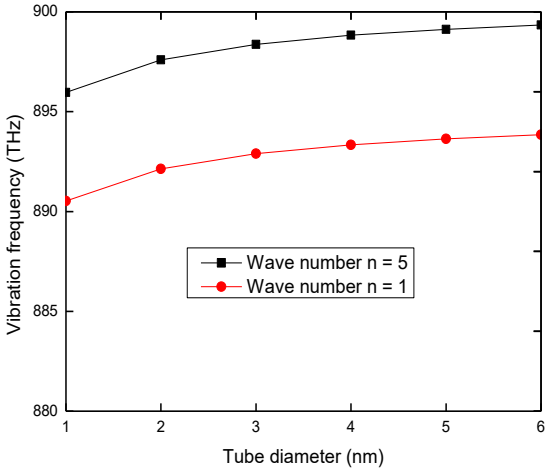

Fig. 5 Response of vibration frequencies (THz) of armchair (5, 5) versus variation of tube diameter (nm) with clamped-clamped edge condition

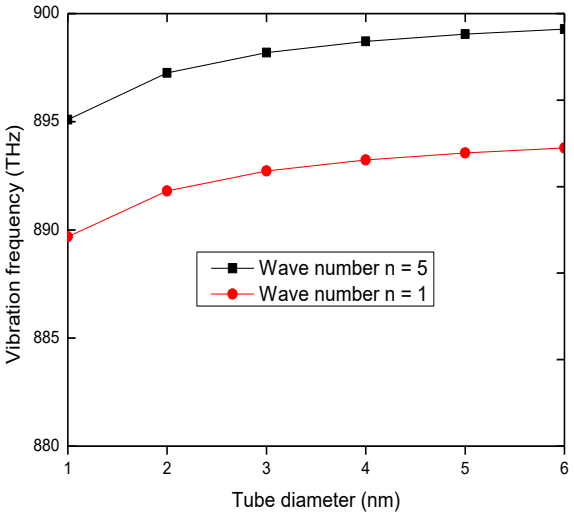

Fig. 4 Response of vibration frequencies (THz) of armchair (5, 5) versus variation of tube diameter (nm) with clamped simply supported edge condition

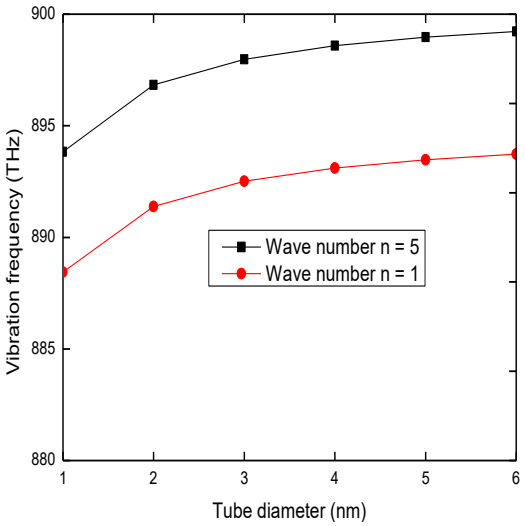

Fig. 6 Response of vibration frequencies (THz) of armchair (5, 5) versus variation of tube diameter (nm) with simply supported edge condition

conditions decreases. It is observed that the natural frequency of $n = 5$ is a little bit greater than $n = 1$ with the variation of values of tube diameters ($d = 1 \sim 6$ nm). The frequency line from ($d = 1 \sim 2$ nm) for both wave number ($n = 1, 5$) and the distance of frequency line from ($d = 2 \sim 3$ nm) suddenly decreases. In this graph, the gap between from $n = 1$and $n = 5$ in start is very small for ($d = 1 \sim 2$ nm). The clamped free frequencies of clamped free is less than that of all other prescribed boundary conditions. The natural frequency rises as d grows, while the frequencies fall as the tube diameter with clamped free boundary conditions decreases. The frequency goes up on increasing the tube diameters with two wave numbers. Effect of increasing the wave number with increasing tube diameter is very interesting. The increment of wave number is same as well as the increment of tube diameter. The frequencies increase on increasing the tube diameter (nm) and increases on increasing the wave number. Also the effect is seen with two different wave numbers. The frequency pattern is different for these two different wave numbers. The frequencies on increasing the wave numbers with values of tube diameter are prominent effect on the vibration of SNTs. It is evident that clamped simply supported frequencies are lower than clamped-clamped frequencies.

It is due to the mathematical formulations of boundary conditions. In Fig. 5, the natural frequencies (THz) of armchair (5, 5) SNTs are sketched with the variation of tube diameter (nm) with clamped-clamped conditions. These frequencies have been calculated for different wave numbers $n = 1, 5$. Both frequency curves increases on increasing the tube diameters. The bend in the curve is maximum from tube diameter ($d = 1 \sim 4$) and smooth increment is seen from $d = 5 \sim 6$. It has been noted that as the wave number increases, so do the frequencies. This decrement is visible in between two curves. Fig. 6 shows the variations of simply supported frequencies versus values

of tube diameter (nm) for DWCNTs. With simply supported boundary conditions, the variation in natural frequency has been observed to be significantly influenced by tube diameter (d). Wave numbers n = 1 and 5 correspond to the natural frequencies (THz) for tube diameters d = 1 to 6 nm. With increase in values of d, the frequency increases fast in the beginning but gets slower as the tube get slower from d = 3 ~ 6GPa. It is noted that on decreasing the wave number from n = 5 to 1, the frequencies increases. The collective effective of tube diameter with increasing of wave number is seen, which is great effect for vibration of SNTs. The frequency curves seem like as an arc. The simply supported frequency curves are lower than that of simply supported and clamped-clamped boundary conditions.

5. Conclusions

This work uses an orthotropic model to investigate the vibration of armchair (5, 5) single-walled carbon nanotubes. The partial differential equations that make up the governing equation are often solved approximately. To obtain accurate outcomes, methods that are reliable and effective are preferred. The tube frequency equation is created by using the wave propagation process. It is possible to observe the effect of natural frequencies as tube diameter varies. Four distinct boundary conditions are used to examine the effects of the two different wave numbers. The frequency initially climbs and reaches its maximum value as the tube diameter grows. It is noted that frequency increases as wave numbers rise. Plotting of the variances versus various tube diameter values has also been done. The results of frequencies using the current model match previous calculations quite well.

Acknowledgement

This project was funded by the Deanship of Scientific Research (DSR) at King Abdulaziz University, Jeddah under grant no (GPIP: 781-135-2024). The authors, therefore, acknowledge with thanks DSR for technical and financial support.

References

Akbaş, Ş.D. (2020), "Modal analysis of viscoelastic nanorods under an axially harmonic load", *Adv. Nano Res.*, **8**(4), 277. https://doi.org/10.12989/anr.2020.8.4.277

Ansari, R., Hemmatnezhad, M. and Rezapour, J. (2011), "The thermal effect on nonlinear oscillations of carbon nanotubes with arbitrary boundary conditions", *Curr. Appl. Phys.*, **11**(3), 692-697. https://doi.org/10.1016/j.cap.2010.11.034.

Benmansour, D.L., Kaci, A., Bousahla, A.A., Heireche, H., Tounsi, A., Alwabli, A.S., Alhebshi, A.M., Al-ghmady, K. and Mahmoud, S.R. (2019), "The nano scale bending and dynamic properties of isolated protein microtubules based on modified strain gradient theory", *Adv. Nano Res.*, **7**(6), 443. https://doi.org/10.12989/anr.2019.7.6.443

Bensattalah, T., Zidour, M. and Daouadji, T.H. (2019), "A new nonlocal beam model for free vibration analysis of chiral single-walled carbon nanotubes", *Compos. Mater. Eng*, **1**(1), 21-31. https://doi.org/10.12989/cme.2019.1.1.021

Besseghier, A., Heireche, H., Bousahla, A.A., Tounsi, A. and Benzair, A., (2015), "Nonlinear vibration properties of a zigzag single-walled carbon nanotube embedded in a polymer matrix", *Adv. Nano Res.*, **3**(1), 29. https://doi.org/10.12989/anr.2015.3.1.029

Cao, X., Zhou, J., Zhou, X., Wang, Z., Wang, Z. and Sheng, Y. (2024), "Experimental research on the synergy effect of resistance/inhibition on the syngas explosion", *Fuel*, **363**, 130995. https://doi.org/10.1016/j.fuel.2024.130995

Ebrahimi F. and Mahmoodi, F. (2018), "Vibration analysis of carbon nanotubes with multiple cracks in thermal environment", *Adv Nano Res*, **6**(1), 57-80. https://doi.org/10.12989/anr.2018.6.1.057

Ebrahimi, R. (2022), "Chaotic vibrations of carbon nanotubes subjected to a traversing force considering nonlocal elasticity theory", *Proceedings of the Institution of Mechanical Engineers, Part N: Journal of Nanomaterials, Nanoengineering and Nanosystems*, **236**(1-2), 31-40. https://doi.org/10.1177/2397791421106330

Fakhrabadi, M.M.S., Rastgoo, A. and Ahmadian, M.T. (2015), "Application of electrostatically actuated carbon nanotubes in nanofluidic and bio-nanofluidic sensors and actuators", *Measurement*, **73**, 127-136. https://doi.org/10.1016/j.measurement.2015.05.009

Fatahi-Vajari, A., Azimzadeh, Z. and Hussain, M. (2019), "Nonlinear coupled axial-torsional vibration of single-walled carbon nanotubes using homotopy perturbation method", *Micro Nano Lett.*, **14**(14), 1366-1371. https://doi.org/10.1049/mnl.2019.0203

Flügge, W. (1962), *Statik und Dynamik der Scahlen*, Springer, Berlin, Germany.

Flügge, W. (2013), *Stresses in Shells*, Springer Science and Business Media.

Forsat, M., Musharavati, F., Eltai, E., Zain, A.M., Mobayen, S. and Mohamed, A.M. (2021), "Vibration characteristics of microplates with GNPs-reinforced epoxy core bonded to piezoelectric-reinforced CNTs patches", *Adv. Nano Res.*, **11**(2), 115. https://doi.org/10.12989/anr.2021.11.2.115

Ghasemi, S.E. and Gouran, S. (2022), "Nonlinear analysis on flow-induced vibration of single-walled carbon nanotubes employing analytical methods", *Int. J. Struct. Stabil. Dyn.*, 2250115. https://doi.org/10.1142/S0219455422501152

Hernandez, E., Goze, C., Bemier, P. and Rubio, A. (1998), "Elastic properties of C and $B_xC_yN_z$ composite nanotubes", *Phys. Rev. Lett*, **80**, 4502-505. https://doi.org/10.1103/PhysRevLett.80.4502.

Hu, Y.G., Liew, K.M., Wang, Q., He, X.Q. and Yakobson, B.I. (2008), "Nonlocal shell model for elastic wave propagation in single- and double-walled carbon nanotubes", *J. Mech. Phys. Solids*, **56**, 3475-3485. https://doi.org/10.1016/j.jmps.2008.08.010

Iijima, S. (1991), "Helical microtubules of graphitic carbon", *Nature*, **354**(6348), 56-58. https://doi.org/10.1038/354056a0

Ipek, C., Sofiyev, A., Fantuzzi, N. and Efendiyeva, S.P. (2023), "Buckling behavior of nanocomposite plates with functionally graded properties under compressive loads in elastic and thermal environments", *J. Appl. Comput. Mech.*, **9**(4), 974-986. https://doi.org/10.22055/jacm.2023.43091.4019

Jena, S.K., Chakraverty, S., Malikan, M. and Mohammad-Sedighi, H. (2020), "Hygro-magnetic vibration of the single-walled carbon nanotube with nonlinear temperature distribution based on a modified beam theory and nonlocal strain gradient model", *Int. J. Appl. Mech.*, **12**(5), 2050054. https://doi.org/10.1142/S1758825120500544

Jena, S.K., Chakraverty, S., Malikan, M. and Mohammad-Sedighi,

H. (2020), "Hygro-magnetic vibration of the single-walled carbon nanotube with nonlinear temperature distribution based on a modified beam theory and nonlocal strain gradient model", *Int. J. Appl. Mech.*, **12**(5), 2050054. https://doi.org/10.1142/S1758825120500544

Kumar, B.R. (2018), "Investigation on mechanical vibration of double-walled carbon nanotubes with inter-tube Van der waals forces", *Adv. Nano Res.*, **6**(2), 135. https://doi.org/10.12989/anr.2018.6.2.135

Lin, L., Ma, X., Chen, C., Xu, J. and Huang, N. (2024), "Imbalanced industrial load identification based on optimized CatBoost with entropy features", *J. Electr. Eng. Technol.*, **19**(8), 4817-4832. https://doi.org/10.1007/s42835-024-01933-5

Luo, J., Lv, M., Hou, S., Nasihatgozar, M. and Behshad, A. (2022), "Dynamic analysis of viscoelastic concrete plates containing nanoparticle subjected to low velocity impact load", *Adv. Nano Res.*, **13**(4), 369-378. https://doi.org/10.12989/anr.2022.13.4.369

Malikan, M. and Eremeyev, V.A. (2020), "Post-critical buckling of truncated conical carbon nanotubes considering surface effects embedding in a nonlinear Winkler substrate using the Rayleigh-Ritz method", *Mater. Res. Express*, **7**(2), 025005. https://doi.org/10.1088/2053-1591/ab691c

Meng, X., Lin, L., Li, H., Chen, Y. and Mei, H. (2024a), "Characteristics of streamer discharge along the insulation surface with embedded electrode", *IEEE T Dielectr. Electr. Insulat.*, **31**(4), 2038-2044. https://doi.org/10.1109/TDEI.2024.3394833

Meng, X., Zhang, B., Cao, F. and Liao, Y. (2024b), "Effectiveness of measures on natural gas pipelines for mitigating the influence of DC ground current", *IEEE T Power Deliv.*, **39**(4), 2414-2423. https://doi.org/10.1109/TPWRD.2024.3406826

Miyashiro, D., Hamano, R., Taira, H. and Umemura, K. (2021), "Analysis of vibration behavior in single strand DNA-wrapped single-walled carbon nanotubes adhered to lipid membranes", *Forces Mech.*, **2**, 100008. https://doi.org/10.1016/j.finmec.2020.100008

Moradi, Z., Ebrahimi, F. and Davoudi, M. (2023), "Vibration control, energy harvesting and forced vibration of the piezoelectric NEMS via paradox-free local/nonlocal theory", *Adv. Nano Res.*, **14**(4), 335-353. https://doi.org/10.12989/anr.2023.14.4.335

Naidu, S.S., Varun, C. and Satyanarayana, G. (2012), "Fundamental natural frequencies of double-walled carbon with different boundary conditions", *Int. J. Eng. Res. Technol.*, **1**(10).

Natsuki, T., Lei, X.W., Ni, Q.Q. and Endo, M. (2010), "Free vibration characteristics of double-walled carbon nanotubes embedded in an elastic medium", *Phys. Lett. A*, **374**(26), 2670-2674. https://doi.org/10.1016/j.physleta.2010.04.040

Ponnusamy, P. and Amuthalakshmi, A. (2013), "Vibration analysis of a viscous fluid conveying double walled carbon nanotube", *Proceedings of the International Conference on Advanced Nanomaterials and Emerging Engineering Technologies*, 231-236. https://doi.org/10.1109/ICANMEET.2013.6609285.

Pourasghar, A., Yang, W., Brigham, J. and Chen, Z. (2021), "Nonlocal thermoelasticity: Transient heat conduction effects on the linear and nonlinear vibration of single-walled carbon nanotubes", *Mech. Based Des. Struct.*, 1-17. https://doi.org/10.1080/15397734.2021.1985516

Qian, D., Wagner, G.J., Liu, W.K., Yu, M.F. and Ruoff, R.S. (2002), "Mechanics of carbon nanotubes", *Appl. Mech. Rev*, **55**(6), 495-533.https://doi.org/10.1115/1.1490129.

Safaei, B., Khoda, F.H. and Fattahi, A.M. (2019), "Non-classical plate model for single-layered graphene sheet for axial buckling", *Adv. Nano. Res.*, **7**(4), 265-275. https://doi.org/10.12989/anr.2019.7.4.265

Sedighi, H.M. and Daneshmand, F. (2014), "Static and dynamic pull-in instability of multi-walled carbon nanotube probes by He's iteration perturbation method", *J. Mech. Sci. Technol.*, **28**, 3459-3469. https://doi.org/10.1007/s12206-014-0807-x

Sosa, E.D., Darlington, T.K., Hanos, B.A. and O'Rourke, M.J.E. (2014), "Multifunctional thermally remendable nanocomposites", *J. Compos.*, 705687. http://doi.org/10.1155/2014/705687

Strozzi, M., Manevitch, L.I., Pellicano, F., Smirnov, V.V. and Shepelev, D.S. (2014), "Low-frequency linear vibrations of single-walled carbon nanotubes: Analytical and numerical models", *J. Sound Vib.*, **333**(13), 2936-2957. https://doi.org/10.1016/j.jsv.2014.01.016

Shang, T., Chen, B., Yanling, W., Ting, Y., Hailiang, L. and Lixin, W. (2024), "Identification of aircraft longitudinal aerodynamic parameters using an online corrective test for wind tunnel virtual flight", *Chinese J. Aeronaut.*, **37**(9), 261-275. https://doi.org/10.1016/j.cja.2024.05.031

Tokio, Y. (1995), "Recent development of carbon nanotube", *Synth. Met.*, **70**, 1511-8. https://doi.org/10.1016/0379-6779(94)02939-V

Tylikowski, A. (2008), "Instability of thermally induced vibrations of carbon nanotubes", *Arch. Appl. Mech.*, **78**, 49-60. https://doi.org/10.1007/s00419-007-0140-2

Wang, B.L. and Wang, K.F. (2013), "Vibration analysis of embedded nanotubes using nonlocal continuum theory", *Compos. Part B Eng.*, **47**, 96-101. https://doi.org/10.1016/j.compositesb.2012.10.043

Wang, H., Sun, W., Jiang, D. and Qu, R. (2023), "A MTPA and flux-weakening curve identification method based on physics-informed network without calibration", *IEEE T Power Electr.*, **38**(10), 12370-12375. https://doi.org/10.1109/TPEL.2023.3295913

Wang, J., Bai, L., Fang, Z., Han, R., Wang, J. and Choi, J. (2024), "Age of information based URLLC transmission for UAVs on pylon turn", *IEEE T Vehicul. Technol.*, **73**(6), 8797-8809. https://doi.org/10.1109/TVT.2024.3358844

Wang, Q., Chen, L., Xiao, G., Wang, P., Gu, Y. and Lu, J. (2024), "Elevator fault diagnosis based on digital twin and PINNs-e-RGCN", *Sci. Rep.*, **14**(1), 30713. https://doi.org/10.1038/s41598-024-78784-7

Wang, Z., Li, J., Yuan, Y., Zhang, S., Hu, W., Ma, J. and Tan, J. (2025b), "Digital-twin-enabled online wrinkling monitoring of metal tube bending manufacturing: A multi-fidelity approach using forward-convolution-GAN", *Appl. Soft Comput.*, **171**, 112684. https://doi.org/10.1016/j.asoc.2024.112684

Wang, Z., Yang, Y., Parastesh, F., Cao, S. and Wang, J. (2025a), "Chaotic dynamics of a carbon nanotube oscillator with symmetry-breaking", *Physica Scripta*, **100**(1), 015225. https://doi.org/10.1088/1402-4896/ad9552

Xiaoming, Z., Shuo, S. and Jiangong, Y. (2025), "Dispersion characteristics of Lamb wave in a multilayered magnetoelectro-elastic plate with an imperfect interface", *J. Intell. Mater. Syst. Struct.*, 1-15. https://doi.org/10.1177/1045389X241306779

Xu, K.U., Aifantis, E.C. and Yan, Y.H. (2008), "Vibrations of double-walled carbon nanotubes with different boundary conditions between inner and outer tubes", *J. Appl. Mech.*, **75**(2), 021013-1. https://doi.org/10.1115/1.2793133.

Xu, X. and Li, B. (2024), "PDE-based observation and predictor-based control for linear systems with distributed infinite input and output delays", *Automatica*, **170**, 111845. https://doi.org/10.1016/j.automatica.2024.111845

Xu, X. and Li, B. (2025), "Semi-global stabilization of parabolic PDE-ODE systems with input saturation", *Automatica*, **171**, 111931. https://doi.org/10.1016/j.automatica.2024.111931

Yang, Q., Li, H., Zhang, L., Guo, K. and Li, K. (2024), "Nonlinear flutter in a wind-excited double-deck truss girder bridge: experimental investigation and modeling approach", *Nonlinear Dyn.*, 1-19. https://doi.org/10.1007/s11071-024-10496-z

Yang, Q., Zeng, X., Guo, K., Cao, S., Wei, K., Shan, W. and

Tamura, Y. (2025), "Analysis of vortex-induced vibration in flexible risers using a physically-meaningful wake-oscillator model", *Eng. Struct.*, **325**, 119415. https://doi.org/10.1016/j.engstruct.2024.119415

Yoon, J. (2006), "Elastic beam models for dynamics of multiwall carbon nanotubes", Thesis, University of Alberta Libraries, Edmonton, Canada. https://era.library.ualberta.ca/items/84b8965d-4877-4c63-881c-3357eb27568f

Yoon, J., Ru, C.Q. and Mioduchowski. A. (2003), "Vibration of an embedded multiwall carbon nanotube", *Compos. Sci. Tech.*, **63**(11), 1533-1542. https://doi.org/10.1016/S0266-3538(03)00058-7.

Yu, H., Wang, H. and Lian, Z. (2022), "An assessment of seal ability of tubing threaded connections: A hybrid empirical-numerical method", *J. Energy Resour. Technol.*, **145**(5). https://doi.org/10.1115/1.4056332

Zeng, W., Zhou, P., Wu, Y., Wu, D. and Xu, M. (2024), "Multi-cavitation states diagnosis of the vortex pump using a combined DT-CWT-VMD and BO-LW-KNN based on motor current signals", *IEEE Sensors J.*, **24**(19), 30690-30705. https://doi.org/10.1109/JSEN.2024.3446170

Zhang, Y.Q., Liu, G.R. and Xie, X.Y. (2005), "Free transverse vibrations of double-walled carbon nanotubes using a theory of nonlocal elasticity", *Phys. Rev. B*, **71**(19), 195404. https://doi.org/10.1103/PhysRevB.71.195404

Zhang, Y.Y., Wang, C.M. and Tan, V.B.C. (2009), "Assessment of Timoshenko beam models for vibrational behavior of single-walled carbon nanotubes using molecular dynamics", *Adv. Appl. Math. Mech.*, **1**, 89-106.

CC